

DETERMINATION OF STELLAR PARAMETERS FOR FGK-DWARF STARS: THE NIR
APPROACH

by

Daniel Thaagaard Andreassen

A thesis submitted in conformity with the requirements
for the degree of Doctor of Philosophy
Graduate Department of Departamento de Física e Astronomia
University of Porto

© Copyright 2017 by Daniel Thaagaard Andreassen

Dedication

To Linnea, Henriette, and Rico

For always supporting me

Acknowledgements

Lorem ipsum dolor sit amet, consectetur adipiscing elit. Ut purus elit, vestibulum ut, placerat ac, adipiscing vitae, felis. Curabitur dictum gravida mauris. Nam arcu libero, nonummy eget, consectetur id, vulputate a, magna. Donec vehicula augue eu neque. Pellentesque habitant morbi tristique senectus et netus et malesuada fames ac turpis egestas. Mauris ut leo. Cras viverra metus rhoncus sem. Nulla et lectus vestibulum urna fringilla ultrices. Phasellus eu tellus sit amet tortor gravida placerat. Integer sapien est, iaculis in, pretium quis, viverra ac, nunc. Praesent eget sem vel leo ultrices bibendum. Aenean faucibus. Morbi dolor nulla, malesuada eu, pulvinar at, mollis ac, nulla. Curabitur auctor semper nulla. Donec varius orci eget risus. Duis nibh mi, congue eu, accumsan eleifend, sagittis quis, diam. Duis eget orci sit amet orci dignissim rutrum.

Nam dui ligula, fringilla a, euismod sodales, sollicitudin vel, wisi. Morbi auctor lorem non justo. Nam lacus libero, pretium at, lobortis vitae, ultricies et, tellus. Donec aliquet, tortor sed accumsan bibendum, erat ligula aliquet magna, vitae ornare odio metus a mi. Morbi ac orci et nisl hendrerit mollis. Suspendisse ut massa. Cras nec ante. Pellentesque a nulla. Cum sociis natoque penatibus et magnis dis parturient montes, nascetur ridiculus mus. Aliquam tincidunt urna. Nulla ullamcorper vestibulum turpis. Pellentesque cursus luctus mauris.

Abstract

Nam dui ligula, fringilla a, euismod sodales, sollicitudin vel, wisi. Morbi auctor lorem non justo. Nam lacus libero, pretium at, lobortis vitae, ultricies et, tellus. Donec aliquet, tortor sed accumsan bibendum, erat ligula aliquet magna, vitae ornare odio metus a mi. Morbi ac orci et nisl hendrerit mollis. Suspendisse ut massa. Cras nec ante. Pellentesque a nulla. Cum sociis natoque penatibus et magnis dis parturient montes, nascetur ridiculus mus. Aliquam tincidunt urna. Nulla ullamcorper vestibulum turpis. Pellentesque cursus luctus mauris.

Resumo

Nam dui ligula, fringilla a, euismod sodales, sollicitudin vel, wisi. Morbi auctor lorem non justo. Nam lacus libero, pretium at, lobortis vitae, ultricies et, tellus. Donec aliquet, tortor sed accumsan bibendum, erat ligula aliquet magna, vitae ornare odio metus a mi. Morbi ac orci et nisl hendrerit mollis. Suspendisse ut massa. Cras nec ante. Pellentesque a nulla. Cum sociis natoque penatibus et magnis dis parturient montes, nascetur ridiculus mus. Aliquam tincidunt urna. Nulla ullamcorper vestibulum turpis. Pellentesque cursus luctus mauris.

Contents

List of Tables	viii
List of Figures	ix
1 Introduction	1
1.1 Exoplanets	1
1.1.1 Detecting exoplanets	1
1.1.1.1 Transit method	2
1.1.1.2 Radial velocity method	3
1.1.1.3 Direct imaging	4
1.1.1.4 Astrometry	4
1.1.1.5 Transit timing variation	4
1.1.1.6 Microlensing	4
1.1.2 Towards the Earth twin	5
1.2 Planet host stars	6
1.3 Applications from knowing the stars	6
1.4 This thesis	6
2 Theory	7
2.1 Stellar structure	7
2.2 Stellar atmosphere	8
2.2.1 Atmosphere models	10
2.2.2 Radiative transfer code - MOOG	12
2.2.3 The equivalent width	12
2.2.3.1 Temperature dependence	12
2.2.3.2 Pressure dependence	13
2.2.3.3 Abundance dependence	15
2.2.3.4 Microturbulence	18
2.3 Line list and atomic data	19
2.4 Spectrographs	19
3 Deriving stellar parameters	21
3.1 Photometry	21
3.1.1 InfraRed Flux Method - IRFM	21

3.1.2	T_{eff} -colour-[Fe /H] calibration	22
3.1.3	Asteroseismology	23
3.2	Spectroscopy	24
3.2.1	Synthesis	24
3.3	FASMA	25
3.3.1	Ingredients	25
3.3.2	Wrapper for ARES	26
3.3.3	Interpolation of atmosphere models	27
3.3.4	Minimization	28
3.3.5	Error estimate	31
4	Results for FGK stars	32
4.1	The creation of a NIR line list	32
4.1.1	Measuring the EWs and first filtering	33
4.1.2	Visual removal of lines	34
4.1.3	Synthetic investigation	34
4.1.4	Calibrating the line list: astrophysical $\log gf$ values	36
4.1.5	Removal of high dispersion lines	37
4.2	HD20010	38
4.3	The NIR line list - toward cooler stars	41
4.4	HD 20010 - revisited	44
4.5	Arcturus	44
4.6	10 Leo	45
4.7	Synthetic cool stars	47
4.8	Parameter dependence on EP cut	52
5	SWEET-Cat	53
5.1	What is SWEET-Cat?	53
5.2	Data for 50 planet hosts	53
5.2.1	Data collected from proposals	54
5.2.2	Data collected from archive	55
5.3	Analysis of 50 planet hosts	55
5.3.1	Habitable zone	57
5.3.2	Changes to planetary parameters	57
5.3.2.1	HAT-P-46	61
5.3.2.2	HD 120084	61
5.3.2.3	HD 233604	61
5.3.2.4	HD 5583	62
5.3.2.5	HD 81688	62
5.3.2.6	HIP 107773	62
5.3.2.7	WASP-97	63
5.3.2.8	ω Serpentis (ome Ser)	63
5.3.2.9	ϕ Ursa Major (omi UMa)	63
5.4	Discovering two giant planet populations	63

5.5 Updating SWEET-Cat	64
6 Future work	66
A SWEET-Cat update of 50 planet hosts	67
Bibliography	71

List of Tables

4.1	Summary of the four stars used in this thesis. The stellar parameters are an average from the PASTEL catalogue (Soubiran et al., 2016) (see text for details), except the parameters for the Sun.	32
4.2	Selection of literature values for the atmospheric parameters for HD 20010. The mean and a 3σ standard deviation is presented at the end of the table from the literature values included, which was used as a reference for the derived parameters.	38
4.3	The derived parameters for HD20010 with and without fixed surface gravity.	40
4.4	Results for the three stars where first set of parameters are the literature values as presented in Table 4.1, second set of parameters are results with $\log g$ set to the same value during the minimization procedure as found in the literature (fixed), and last set of parameters are with all parameters free during the minimization procedure.	44
5.1	Columns in SWEET-Cat	54
5.2	Spectrographs used for this paper with their spectral resolution, wavelength coverage, and mean S/N from the spectra used.	55
5.3	Host star and planetary properties of GJ 785, HD 37124, and KELT-6; all which have an exoplanet in the habitable zone.	59
A.1	Derived parameters for the 50 stars in our sample. The S/N was measured by ARES. . .	68
A.1	continued.	69
A.1	continued.	70

List of Figures

1.1	<i>Upper plot:</i> The lightcurve of a star with an exoplanet transiting. <i>Lower plot:</i> The phase curve of the above lightcurve.	2
1.2	<i>Upper panel:</i> RV time series of EPIC 9792 from the SOPHIE spectrograph. <i>Lower panel:</i> Phase curve of the time series above, using the period of 3.261 days.	3
1.3	The mass of exoplanet since the detection of the first exoplanet until now. The horizontal lines are the mass of Jupiter (upper), Neptune (middle), and Earth (lower).	5
2.1	Energy levels for hydrogen, $E_n = \frac{-13.6 \text{ eV}}{n^2}$	11
2.2	An absorption line centred at λ_0 normalised at the flux level F_c . The area of the absorption line to the left is equal to the blue shaded area in the rectangle to the right with width EW.	13
2.3	The EW for a Fe I and Fe II line with increasing T_{eff} . The two lines have similar EW in the Sun and are found in the optical part of the spectrum. The vertical line show the solar T_{eff}	14
2.4	<i>Upper panel:</i> Curve of growth for same Fe II used in Figure 2.3 for four different $\log g$ values. Here it is the weak lines mostly affected by the change in $\log g$. <i>Lower left panel:</i> Synthetic spectra of the same line. The colour scale is the same. <i>Lower right:</i> The abundance for the line at different $\log g$. A strong correlation (0.40) is seen.	16
2.5	<i>Upper panel:</i> Curve of growth of the same Fe I line as used in Figure 2.3. Four points are marked which is shown in the <i>lower panel</i> as a synthetic spectral line. The RW (proxy for EW) is clearly increasing with $\log gf$ (proxy for abundance).	17
2.6	Curve of growth for three different values of ξ_{micro} . The EW is increasing with increasing ξ_{micro}	18
3.1	Measured and calculated flux from the Sun at infrared wavelengths. Data from Table 2 in Blackwell and Shallis (1977) . Mean solar radius from this data is $1.011R_{\odot}$, and mean solar $T_{\text{eff}} = 5963 \text{ K}$ using Equation 3.1.	22
3.2	Mass and radius from asteroseismic scaling relation. The colour is the mass and radius for the upper and lower panel, respectively.	24
3.3	Model atmosphere grid from Kurucz (1993) at $[\text{Fe}/\text{H}] = 0.00$ between 3000 K and 10 000 K. The grid extends to higher T_{eff} , but these are not considered in this thesis.	27
3.4	The abundances of Fe I for the planet host star: HATS-1. Upper plot: Converged parameters (see text for stellar parameters for this star). Middle plot: Converged parameters with 0.5 km/s added to ξ_{micro} . Lower plot: Converged parameters with 500 K added to T_{eff}	29
3.5	Overview of the minimization for FASMA. Credit: Andreasen et al. (2017b)	31

4.1	Solar spectrum (blue) with all iron lines in the spectral region (green) and other elements (orange). The depths and transparencies of the vertical lines are a measure of the line strengths (see Equation 4.1 for details). This is a case where the iron line is discarded due to blending, which is clear in the left wing of the central absorption line.	35
4.2	The three coloured curves represent different iron abundance, $\{-0.20; 0.00; 0.20\}$ compared to solar abundance. The grey curve is the solar atlas for reference. In this case the iron line at $15\,550.439\text{ \AA}$ was investigated. <i>Upper panel</i> : Synthetic spectra were computed using the full VALD line list in the spectral range for the three different iron abundances. <i>Lower panel</i> : Same as the upper panel, but with the iron line removed from the line list. Since the synthetic spectra shows no features at this absorption line anymore, it is a fair assumption to say the iron line is the cause of this absorption line.	35
4.3	Line abundance of all iron lines before calibrating the $\log gf$ values. The green points are the points with a deviation less than 1.0 dex from the solar iron abundance. All the red points are discarded. The horizontal line shows the solar iron abundance.	36
4.4	The most disperse lines. <i>Upper panel</i> : The MAD versus the original EW. The red points are the outliers which were discarded during this process. <i>Lower plot</i> : Same as above with the de-trended MAD by the exponential fit as shown in the upper panel.	38
4.5	Line identification in piece of Arcturus spectrum with PHOENIX model and telluric model for correcting RV.	40
4.6	Difference in abundance for HD 20010 when multiple measurements of EW were obtained. The differences are between the lowest and highest measured EW in case of multiple measurements. This is shown against the wavelength (<i>upper panel</i>) and in a histogram (<i>lower panel</i>).	41
4.7	Comparison of the EW from the first version of the line list, EW_1 , and the second version, EW_2 . The EWs are generally higher in the second version, with an average difference between the two version of $(2.1 \pm 11.1)\text{ m\AA}$. The three horizontal lines show the average value and the standard deviation.	43
4.8	Top figure: Difference of the automatic EW measurements between the summer observations and winter observations from the Arcturus spectra. Bottom figure: Same as above, but with manual measurements from ARES (summer) and automatic measurements (summer).	46
4.9	Derived parameters of 12 synthetic PHOENIX spectra with varying T_{eff}	48
4.10	Derived parameters of 12 synthetic PHOENIX spectra with varying T_{eff} . Here $\log g$ is fixed at 4.5 dex and ξ_{micro} fixed according to an empirical relation, thus only deriving T_{eff} and $[\text{Fe}/\text{H}]$	49
4.11	Common EWs between Arcturus and the synthetic spectrum with closest parameters (see text for details). The EWs are getting more disperse with increasing EW which is expected when seeing the direct comparison of the spectrum in Figure 4.12.	50
4.12	Comparison between the Arcturus atlas and a PHOENIX synthetic spectrum with similar parameters to Arcturus (see text for details).	50
4.13	Derived $[\text{Fe}/\text{H}]$ with respect to the true T_{eff} for runs that reached convergence. <i>Top panel</i> : $\log g$ fixed at 4.5 dex and ξ_{micro} to the empirical relation (see text for details). <i>Lower panel</i> : All parameters free.	51

5.1	A Hertzsprung-Russell diagram of the sample of 50 planet host stars added to SWEET-Cat. The parameters were derived using optical high resolution and high S/N spectra in tandem with FASMA and an optical line list. The colour scale shows the derived $\log g$ for each star.	56
5.2	The habitable zone for the updated SWEET-Cat stars. The coloured line shows the theoretical habitable zone, while the dots shows the location of the planets in the actual system. The blue lines show the habitable zone of the three stars where a planet is located within it (green points). The red dots and orange lines are systems which does not lie within the habitable zone. Finally, the green line shows the location of the Sun's habitable zone and the first five planets placement. In this model both Earth and Mars are within the habitable zone.	58
5.3	Stellar radius on both axes calculated based on Torres et al. (2010) . The x-axis shows the stellar radius based on the atmospheric parameters from the literature, while the y-axis indicates the new homogeneous parameters presented here. The colour and size indicate the surface gravity. This clearly shows that the disagreement is biggest for more evolved stars.	60
5.4	Giant planet masses for the full sample and constrained sample (see text for details). This study was performed by Santos et al. (2017) to distinct two giant planet populations. . . .	64

Chapter 1

Introduction

Ever since the dawn of time, the humankind have looked at the stars and wondered if we are alone in this Universe. To answer this question, one must look toward the field of extrasolar planets (exoplanets). This is a rapidly growing field in astronomy and science in general. Since the first confirmed discovery of an exoplanet around a millisecond pulsar in 1992 by [Wolszczan and Frail \(1992\)](#) and three years later, the more interesting exoplanet 51 Peg b discovered around a solar-type star by [Mayor and Queloz \(1995\)](#), more than 3600 exoplanets have been discovered at the time of writing, July 2017¹.

With the discoveries of exoplanets, the main focus is now mainly on finding the twin of Earth, that is a planet that can harbour life as we know it. However, it is not enough to simply discover small rocky exoplanets. Accurate and precise determination of the stellar parameters are crucial as the planetary parameters (radius, mass, bulk density, etc.) are directly derived from their host's parameters.

In this chapter there will be a general introduction to exoplanets, detection methods, and characterisation (Section 1.1). Then a throughout introduction on the exoplanet host stars (Section 1.2), which is the main focus on this thesis. While learning about host stars, and stars in general, the results have wide-spread applications, where some will briefly be discussed in the end of this chapter (Section 1.3) before an introduction on what this thesis will consists of (Section 1.4).

1.1 Exoplanets

The holy grail in the field of exoplanets is to find the first exoplanet with life. This is by no means an easy task. To give an idea of the difficulty of detecting life on an exoplanet, one must understand all the difficulties to simply detect and confirm an exoplanet. This will shortly be described in the sections below

1.1.1 Detecting exoplanets

There are sex ways of detecting exoplanets, some with advantages over others. In combination with each other, one can potentially learn a lot about the exoplanet(s).

It is important to note, that different things might mimic planetary signals, however they will not be described in this thesis. The confirmation of an exoplanet often happen, when two techniques are able to detect the same exoplanet.

¹ <http://exoplanet.eu/>

1.1.1.1 Transit method

The most successful method, if based on numbers of exoplanets detected, is the transit method. This is a well-known method in astronomy, however only used in the last decade for detecting exoplanets. Before this, it has been used extensively for finding and characterising binary stars. The difference here is, that the exoplanet does not radiate (or at least very little radiation). An example of an exoplanet transiting a star can be seen in Figure 1.1.

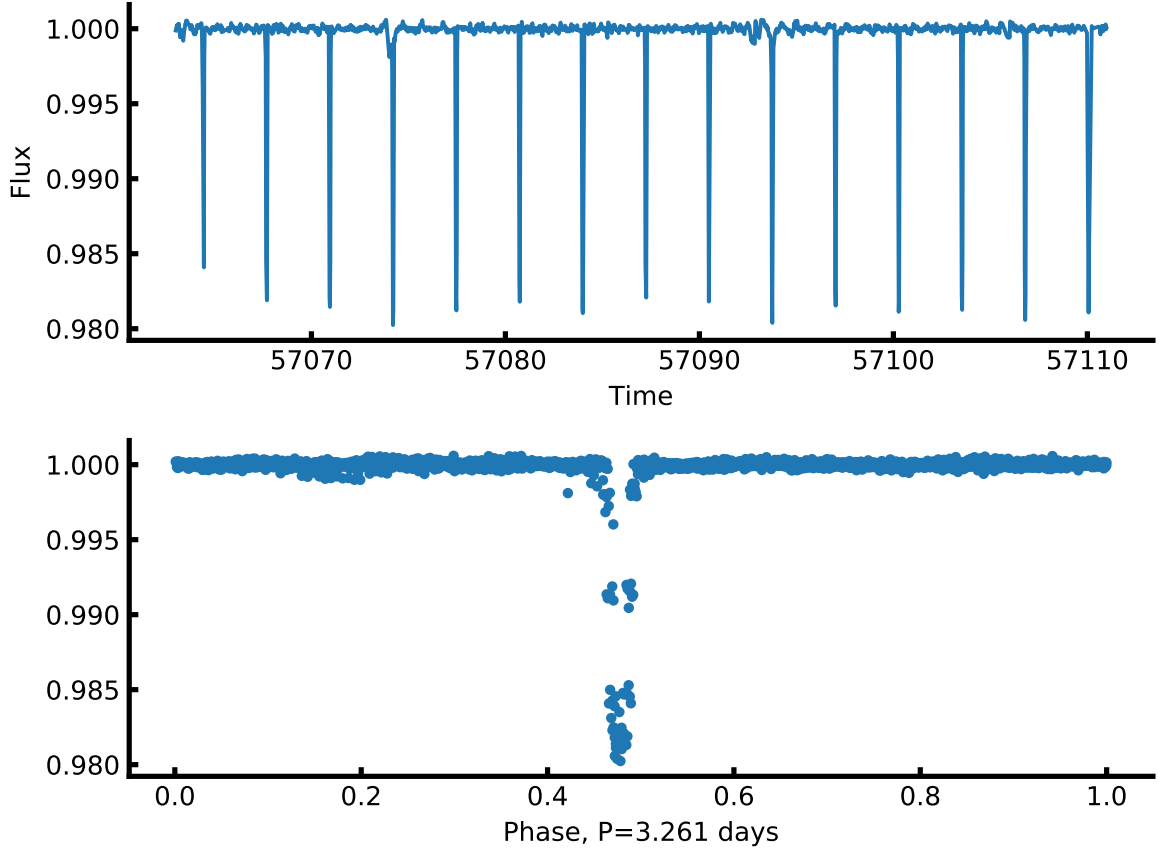


Figure 1.1: *Upper plot:* The lightcurve of a star with an exoplanet transiting. *Lower plot:* The phase curve of the above lightcurve.

As an exoplanet orbit a star, it might transit its host as seen from an observer here on Earth. This signal might be detected if the star's brightness is being monitored as a periodic signal. The decrease in brightness as the planet transit the star is directly related to ration between the stellar radius R_* and the planetary radius R_p :

$$k = \sqrt{\frac{R_p}{R_*}}, \quad (1.1)$$

where k is the depth of the transit compared to the total stellar brightness.

It is possible to obtain the radius of an exoplanet with this method. However, detailed analysis of the phase curve of an exoplanet can reveal the surface temperature of the exoplanet. The transit described

above is also known as the primary transit. If it is possible to detect the secondary transit, that is when the exoplanet goes behind the star as seen from Earth, the difference in light (planet + star right before secondary transit compared to just star) gives the flux of the planet and thus the surface temperature. This is a difficult task as secondary transits are intrinsic faint.

1.1.1.2 Radial velocity method

The radial velocity method is the indirect study of the motion of the host star using the Doppler effect caused by an orbiting exoplanet. This together with the transit method described above is by far the most successful methods to detect and characterise exoplanets. The periodic signal created by the exoplanet on the host star depends on the mass ratio between the star M_* and the planet M_p :

$$K = \frac{28.4329 \text{ km/s}}{\sqrt{1-e^2}} \frac{M_p \sin i}{M_{\text{Jup}}} \left(\frac{M_* + M_p}{M_\odot} \right)^{-2/3} \left(\frac{P}{1 \text{ year}} \right) \quad (1.2)$$

where K is the semi-amplitude of the sinusoidal, e is the eccentricity, i is the inclination, P is the orbital period, and M_{Jup} is the mass of Jupiter. Since $M_* \gg M_p$, the term $M_* + M_p \simeq M_*$ in order to simplify the equation. Often a circular orbit is assumed, $e = 0$. The sinusoidal motion of the star can be seen in Figure 1.2 where both the time series and the phase curve is presented for an exoplanet.

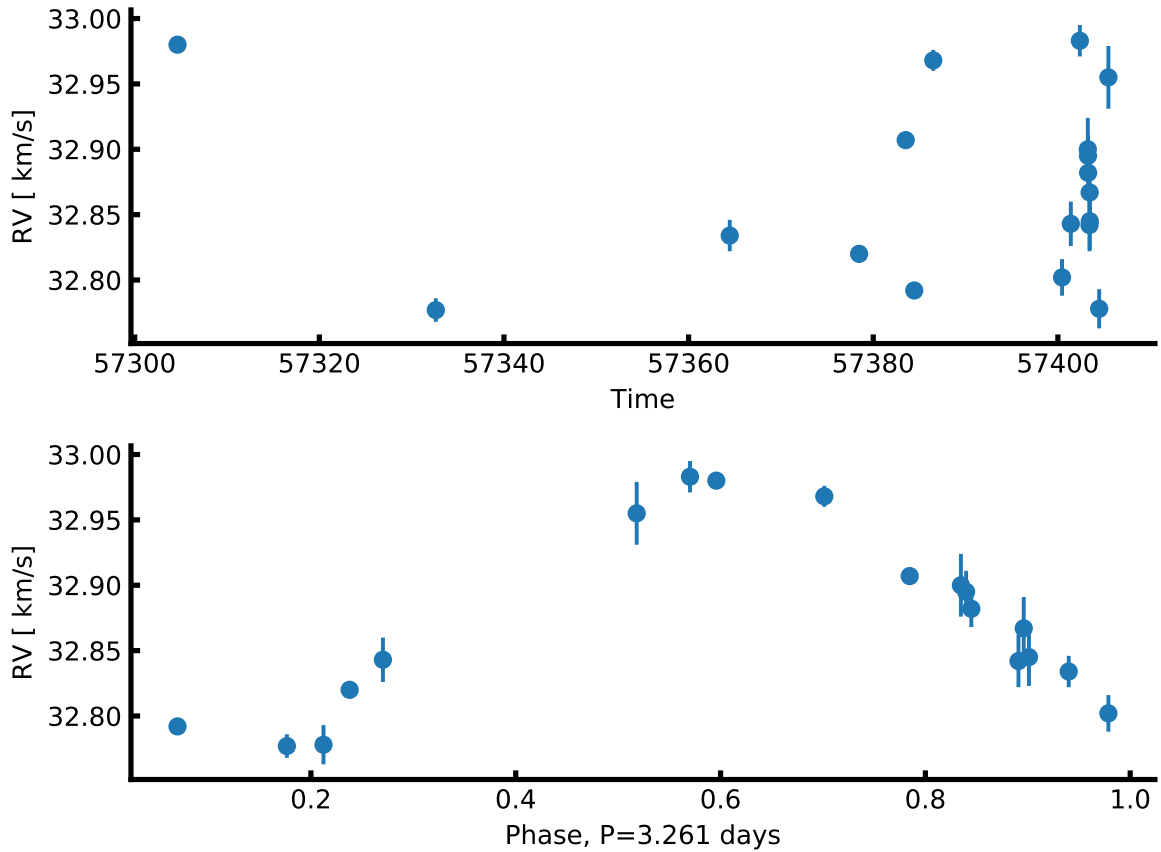


Figure 1.2: *Upper panel:* RV time series of EPIC 9792 from the SOPHIE spectrograph. *Lower panel:* Phase curve of the time series above, using the period of 3.261 days.

In order to apply the radial velocity method for detecting exoplanets, it is necessary to collect spectra, high resolution but often not high S/N, in order to cover most part of the phase of the orbit. These spectra are often combined after the detection of the exoplanet, in order to increase the S/N. This combined spectrum can then be used for characterising the host star.

This method is sensitive to close-in massive exoplanets, also known as hot Jupiters. In combination with the above mentioned transit method, the mass and radius of an exoplanet can be derived, and thus the bulk density which might give hints of the structure and composition of the exoplanet.

1.1.1.3 Direct imaging

Direct imaging is probably the easiest method to understand, however it is quite difficult to actually use this technique. In its core, one has to carefully block the light of a star, and directly imaging the exoplanets around it. However, it is extremely difficult to block the light of the host star and find the reflected light of the exoplanet(s) in orbit.

This technique is sensitive to exoplanets which reflect a lot of light, i.e. a high albedo, and in wide orbits as they are less contaminated by the residual starlight.

1.1.1.4 Astrometry

Using astrometry to detect exoplanets is very similar to the RV method described above in Section 1.1.1.2. Here an observer carefully detect the minute motion of a star caused by an exoplanet. Unlike the RV method, this technique (astrometry) actually looks for changes in the coordinates of the star. This technique has also been used to detect low luminosity stellar companions as e.g. Sirius B.

This technique is sensitive to massive exoplanets as they cause a larger motion compared to lighter companions.

1.1.1.5 Transit timing variation

This technique of detecting exoplanets is a highly indirect method of detecting exoplanets. Here an observer first detect a transiting exoplanet as explained in Section 1.1.1.1. Then variations in the occurrence of mid-transit can be detected if a second non-transiting exoplanet interact with the primary transiting exoplanet (planet-planet interaction). This interaction will periodically course the mid-transit to happen ahead/behind of the time if only one exoplanet would be present.

A careful analysis of the transit timing variations (TTV) can lead to the mass of the secondary non-transiting exoplanet. However, its radius will be unknown. Most of these exoplanets pairs which shows TTV are in an orbital resonant. This technique as well, is more sensitive to massive exoplanets as they will induce a higher signal.

1.1.1.6 Microlensing

This technique is very exotic and not very useful, however since a few exoplanets have been discovered by this technique it deserves a mentioning. The core theory in this technique is the well-known General Relativity. Here an observer looks at a distant star (star A) as a star between the observer and the distant star (star B) passes in front of the line of sight. Star B will act as a microlens and increase the magnitude of star A. This increase of magnitude will reach its maximum as the two stars are most aligned as seen from Earth.

To use this for detecting exoplanet, there will have to be an exoplanet orbiting star B. This act like another lens, momentarily make a secondary increase in magnitude. The amount of increase in magnitude is related to the mass of the exoplanet. The higher the mass, the higher the effect.

While this exotic technique is interesting and has proven successful, it is not very useful as it only occurs once. The stars observed with this technique are often faint, thus making follow-up RV detection very difficult if not impossible with the current instruments.

1.1.2 Towards the Earth twin

The above mentioned techniques will be used to find the Earth twin. Especially will the two first techniques (transit and RV method) be the ones finding the smallest exoplanets as a wide range of instruments are being developed dedicated for this. Since the detection of the first exoplanet around a solar-type star by Mayor and Queloz (1995), the community has been able to detect lower mass exoplanets as seen in Figure 1.3.

Write about
JWST,
Espresso,
NIRPS, etc.

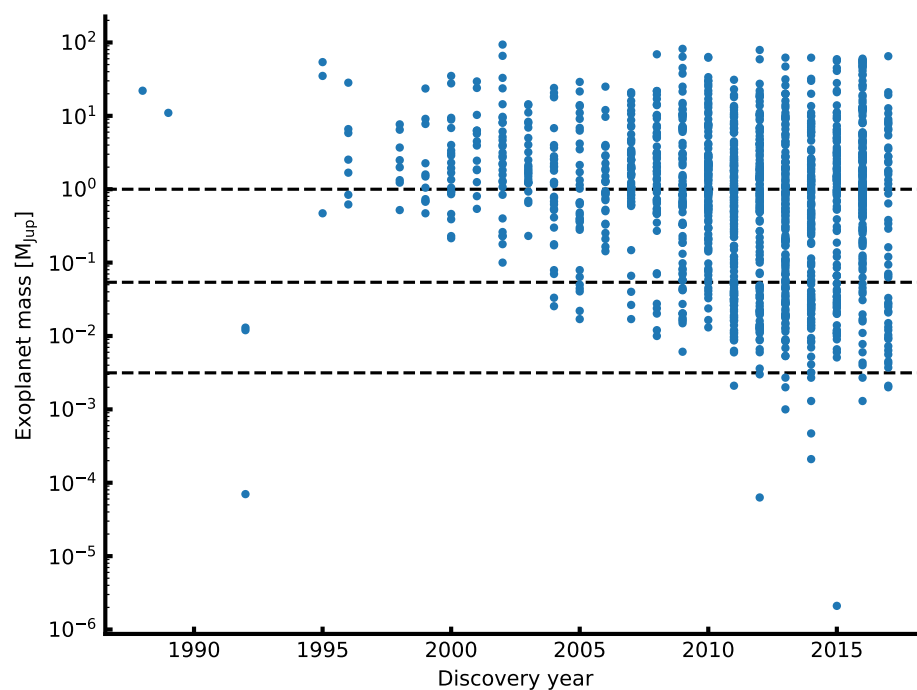


Figure 1.3: The mass of exoplanet since the detection of the first exoplanet until now. The horizontal lines are the mass of Jupiter (upper), Neptune (middle), and Earth (lower).

While the first many discoveries of exoplanets were the, at the time, exotic and strange hot Jupiter like exoplanets in close orbits, the time have come to detect exoplanets with both lower mass and wider orbits. It is crucial to have high precision instruments and long surveys to detect those exoplanets. Missions as *Kepler* and *CoRoT* have been excellent for this, since they have focused on few fields of the sky for a long time.

The first place to look for Earth's twin is around a solar twin. However, since these stars are quite hot, the habitable zone will also be far from the host star. Indeed, to detect a copy of our own solar system we would need to detect the minute signature of an exoplanet in a 1 year orbit around its host

star (a solar twin). If detected with the transit method, more than one transit is needed, hence this will take at least two years, and probably even longer. The endeavour to get the follow-up RV afterwards will also be extremely challenging with today's technology, and only the next generation of spectrographs will be able to detect these signals.

Therefore, it is not a surprise that an effort have been towards detecting Earth-like planets around less massive stars. These stars (M stars) are also colder, hence the habitable zone will be closer to its host compared to the more massive and hotter stars. The nature have been kind, since it seems that the M stars are prone to produce rocky planets rather than giant planets. The shorter period means that the surveys can be shorter for these planets. Moreover, since they are smaller the signal from a transit will be easier to detect (see Equation 1.1). Similarly will the RV signal be larger for an Earth-like planet in the habitable zone around an M star compared to a similar exoplanet around a G star. Both due to the lower period and due to the lower mass of the host star (see Equation 1.2).

The ref. is in the proposals

While M stars seems to be the place to look for the Earth's twin, there are still some challenges to tackle. Foremost is the detailed characterisation of the host star, which are particular troublesome for these stars. This is something that will be focused on in the following section.

1.2 Planet host stars

With the present diversity of exoplanets it becomes increasingly important to get an accurate and precise characterisation of the exoplanets in order to study them in samples and on an individual level. An accurate and precise characterisation can give us an idea whether the planet is rocky, composed of water or gaseous.

1.3 Applications from knowing the stars

1.4 This thesis

Appendix A

SWEET-Cat update of 50 planet hosts

Table A.1: Derived parameters for the 50 stars in our sample. The S/N was measured by ARES.

Star	T_{eff} [K]	$\log g$ [cgs]	[Fe / H]	ξ_{micro} [km/s]	ξ_{micro} fixed?	Instrument	S/N
BD -11 4672	4553 ± 75	4.87 ± 0.51	-0.30 ± 0.02	0.14 ± 0.07	yes	FIES	487
BD +49 828	5015 ± 36	$2.87 \pm 0.09^{\text{a}}$	-0.01 ± 0.03	1.48 ± 0.04	no	FIES	567
GJ 785	5087 ± 48	4.42 ± 0.10	-0.01 ± 0.03	0.69 ± 0.10	no	HARPS	801
HATS-1	5969 ± 46	4.39 ± 0.06	-0.04 ± 0.04	1.06 ± 0.08	no	UVES	155
HATS-5	5383 ± 91	4.41 ± 0.22	0.08 ± 0.06	0.91 ± 0.14	no	UVES	158
HAT-P-12	4642 ± 106	4.53 ± 0.27	-0.26 ± 0.06	0.28 ± 0.63	no	FIES	185
HAT-P-24	6470 ± 181	4.33 ± 0.27	-0.41 ± 0.10	1.40 ± 0.03	yes	UVES	158
HAT-P-39	6745 ± 236	4.39 ± 0.47	-0.21 ± 0.12	1.53 ± 0.04	yes	UVES	127
HAT-P-42	5903 ± 66	$4.29 \pm 0.10^{\text{a}}$	0.34 ± 0.05	1.19 ± 0.08	no	UVES	130
HAT-P-46	6421 ± 121	$4.53 \pm 0.14^{\text{a}}$	0.16 ± 0.09	1.67 ± 0.18	no	UVES	208
HD 120084	4969 ± 40	$2.94 \pm 0.14^{\text{a}}$	0.12 ± 0.03	1.41 ± 0.04	no	ESPaDOnS	852
HD 192263	4946 ± 46	4.61 ± 0.14	-0.05 ± 0.02	0.66 ± 0.12	no	HARPS	415
HD 219134	4767 ± 70	4.57 ± 0.17	0.00 ± 0.04	0.59 ± 0.24	no	ESPaDOnS	725
HD 220842	5999 ± 39	$4.30 \pm 0.06^{\text{a}}$	-0.08 ± 0.03	1.21 ± 0.05	no	FIES	459
HD 233604	4954 ± 46	$2.86 \pm 0.11^{\text{a}}$	-0.14 ± 0.04	1.61 ± 0.05	no	FIES	314
HD 283668	4841 ± 73	4.51 ± 0.18	-0.74 ± 0.04	0.16 ± 0.61	no	FIES	592
HD 285507	4620 ± 126	4.72 ± 0.61	0.04 ± 0.06	0.74 ± 0.43	no	UVES	239
HD 5583	4986 ± 35	$2.87 \pm 0.09^{\text{a}}$	-0.35 ± 0.03	1.62 ± 0.04	no	FIES	933
HD 81688	4903 ± 21	$2.70 \pm 0.05^{\text{a}}$	-0.21 ± 0.02	1.54 ± 0.02	no	^b	1350, 860
HD 82886	5123 ± 18	$3.30 \pm 0.04^{\text{a}}$	-0.25 ± 0.01	1.16 ± 0.02	no	^c	1198, 1294
HD 87883	4917 ± 68	4.53 ± 0.19	0.02 ± 0.03	0.46 ± 0.21	no	ESPaDOnS	753
HIP 107773	4957 ± 49	$2.83 \pm 0.09^{\text{a}}$	0.04 ± 0.04	1.49 ± 0.05	no	UVES	218
HIP 11915	5770 ± 14	4.33 ± 0.03	-0.06 ± 0.01	0.95 ± 0.02	no	HARPS	709
HIP 116454	5042 ± 72	4.69 ± 0.15	-0.16 ± 0.03	0.71 ± 0.17	no	UVES	412

Table A.1: continued.

Star	T_{eff} [K]	$\log g$ [cgs]	[Fe / H]	ξ_{micro} [km/s]	ξ_{micro} fixed?	Instrument	S/N
HR 228	5042 ± 42	$3.30 \pm 0.09^{\text{a}}$	0.07 ± 0.03	1.14 ± 0.04	no	UVES	400
KELT-6	6246 ± 88	$4.22 \pm 0.09^{\text{a}}$	-0.22 ± 0.06	1.66 ± 0.13	no	FIES	374
Kepler-37	5378 ± 53	4.47 ± 0.12	-0.23 ± 0.04	0.58 ± 0.13	no	FIES	205
Kepler-444	5111 ± 43	4.50 ± 0.13	-0.51 ± 0.03	0.37 ± 0.15	no	FIES	675
mu Leo	4605 ± 94	$2.61 \pm 0.26^{\text{a}}$	0.25 ± 0.06	1.64 ± 0.11	no	ESPaDOnS	354
ome Ser	4928 ± 35	$2.69 \pm 0.06^{\text{a}}$	-0.11 ± 0.03	1.55 ± 0.04	no	FIES	1168
omi UMa	5499 ± 52	$3.36 \pm 0.07^{\text{a}}$	-0.01 ± 0.05	1.98 ± 0.06	no	ESPaDOnS	527
Qatar-2	4637 ± 316	4.53 ± 0.62	0.09 ± 0.17	0.63 ± 0.83	no	UVES	97
SAND364	4457 ± 104	$2.26 \pm 0.20^{\text{a}}$	-0.04 ± 0.06	1.60 ± 0.11	no	UVES	220
TYC+1422-614-1	4908 ± 41	$2.90 \pm 0.12^{\text{a}}$	-0.07 ± 0.03	1.57 ± 0.05	no	FIES	506
WASP-37	5917 ± 72	4.25 ± 0.15	-0.23 ± 0.05	0.59 ± 0.13	no	FIES	232
WASP-44	5612 ± 80	4.39 ± 0.30	0.17 ± 0.06	1.32 ± 0.13	no	UVES	125
WASP-52	5197 ± 83	4.55 ± 0.30	0.15 ± 0.05	1.16 ± 0.14	no	UVES	125
WASP-58	6039 ± 55	4.23 ± 0.10	-0.09 ± 0.04	1.12 ± 0.08	no	FIES	310
WASP-61	6265 ± 168	$4.21 \pm 0.21^{\text{a}}$	-0.38 ± 0.11	1.44 ± 0.02	yes	UVES	163
WASP-72	6570 ± 85	4.25 ± 0.13	0.15 ± 0.06	2.30 ± 0.15	no	UVES	174
WASP-73	6203 ± 32	$4.16 \pm 0.06^{\text{a}}$	0.20 ± 0.02	1.66 ± 0.04	np	^d	193,231
WASP-75	6203 ± 46	$4.42 \pm 0.22^{\text{a}}$	0.24 ± 0.03	1.45 ± 0.06	no	UVES	189
WASP-76	6347 ± 52	$4.29 \pm 0.08^{\text{a}}$	0.36 ± 0.04	1.73 ± 0.06	no	UVES	165
WASP-82	6563 ± 55	$4.29 \pm 0.10^{\text{a}}$	0.18 ± 0.04	1.93 ± 0.08	no	UVES	239
WASP-88	6450 ± 61	$4.24 \pm 0.06^{\text{a}}$	0.03 ± 0.04	1.79 ± 0.09	no	UVES	174
WASP-94 A	6259 ± 34	$4.34 \pm 0.07^{\text{a}}$	0.35 ± 0.03	1.50 ± 0.04	no	UVES	356
WASP-94 B	6137 ± 21	$4.42 \pm 0.05^{\text{a}}$	0.33 ± 0.02	1.29 ± 0.03	no	UVES	397
WASP-95	5799 ± 31	$4.29 \pm 0.05^{\text{a}}$	0.22 ± 0.03	1.18 ± 0.04	no	UVES	247
WASP-97	5723 ± 52	4.24 ± 0.07	0.31 ± 0.04	1.03 ± 0.08	no	UVES	219

Table A.1: continued.

Star	T_{eff} [K]	$\log g$ [cgs]	[Fe / H]	ξ_{micro} [km/s]	ξ_{micro} fixed?	Instrument	S/N
WASP-99	6324 ± 89	4.34 ± 0.12	0.27 ± 0.06	1.83 ± 0.12	no	UVES	249
WASP-100	6853 ± 209	$4.15 \pm 0.26^{\text{a}}$	-0.30 ± 0.12	1.87 ± 0.02	yes	UVES	166

^a Spectroscopic $\log g$.

^b Weighted average of ESPaDoNS and FIES results. The parameters are (FIES in parantheses): $T_{\text{eff}} = 4870(4934) \pm 30(29)$, $\log g = 2.50(2.73) \pm 0.14(0.05)$, $[\text{Fe} / \text{H}] = -0.26(-0.19) \pm 0.03(0.02)$, and $\xi_{\text{micro}} = 1.50(1.59) \pm 0.03(0.03)$.

^c Weighted average of ESPaDoNS and FIES results. The parameters are (FIES in parantheses): $T_{\text{eff}} = 5124(5121) \pm 22(29)$, $\log g = 3.30(3.31) \pm 0.05(0.07)$, $[\text{Fe} / \text{H}] = -0.25(-0.24) \pm 0.02(0.02)$, and $\xi_{\text{micro}} = 1.15(1.17) \pm 0.03(0.04)$.

^d Weighted average of UVES and FEROS results. The parameters are (FEROS in parantheses): $T_{\text{eff}} = 6313(6162) \pm 61(37)$, $\log g = 4.26(4.14) \pm 0.15(0.06)$, $[\text{Fe} / \text{H}] = 0.22(0.19) \pm 0.04(0.03)$, and $\xi_{\text{micro}} = 1.85(1.61) \pm 0.08(0.04)$.

Bibliography

- Adamów, M., Niedzielski, A., Villaver, E., Wolszczan, A., and Nowak, G.: 2014, *A&A* **569**, A55
- Adibekyan, V., Delgado-Mena, E., Figueira, P., Sousa, S. G., Santos, N. C., González Hernández, J. I., Minchev, I., Faria, J. P., Israelian, G., Harutyunyan, G., Suárez-Andrés, L., and Hakobyan, A. A.: 2016, *A&A* **592**, A87
- Adibekyan, V. Z., Benamati, L., Santos, N. C., Alves, S., Lovis, C., Udry, S., Israelian, G., Sousa, S. G., Tsantaki, M., Mortier, A., Sozzetti, A., and De Medeiros, J. R.: 2015, *MNRAS* **450**, 1900
- Adibekyan, V. Z., Figueira, P., Santos, N. C., Mortier, A., Mordasini, C., Delgado Mena, E., Sousa, S. G., Correia, A. C. M., Israelian, G., and Oshagh, M.: 2013, *A&A* **560**, A51
- Aerts, C., Christensen-Dalsgaard, J., and Kurtz, D. W.: 2010, *Asteroseismology*, Springer-Verlag
- Andreasen, D. T., Sousa, S. G., Delgado Mena, E., Santos, N. C., Lebzelter, T., Mucciarelli, A., and Neil, J. J.: 2017a, *A&A* **585**, A143
- Andreasen, D. T., Sousa, S. G., Delgado Mena, E., Santos, N. C., Tsantaki, M., Rojas-Ayala, B., and Neves, V.: 2016, *A&A* **585**, A143
- Andreasen, D. T., Sousa, S. G., Tsantaki, M., Teixeira, G. D. C., Mortier, A., Santos, N. C., Suárez-Andrés, L., Delgado Mena, E., and Ferreira, A. C. S.: 2017b, *A&A* **600**, A69
- Balachandran, S.: 1990, *ApJ* **354**, 310
- Bedding, T. R., Mosser, B., Huber, D., Montalbán, J., Beck, P., Christensen-Dalsgaard, J., Elsworth, Y. P., García, R. A., Miglio, A., Stello, D., White, T. R., De Ridder, J., Hekker, S., Aerts, C., Barban, C., Belkacem, K., Broomhall, A.-M., Brown, T. M., Buzasi, D. L., Carrier, F., Chaplin, W. J., di Mauro, M. P., Dupret, M.-A., Frandsen, S., Gilliland, R. L., Goupil, M.-J., Jenkins, J. M., Kallinger, T., Kawaler, S., Kjeldsen, H., Mathur, S., Noels, A., Silva Aguirre, V., and Ventura, P.: 2011, *Nature* **471**, 608
- Bertaux, J. L., Lalletment, R., Ferron, S., Boonne, C., and Bodichon, R.: 2014, *A&A* **564**, A46
- Blackwell, D. E. and Shallis, M. J.: 1977, *MNRAS* **180**, 177
- Bochanski, J. J., Hawley, S. L., Covey, K. R., West, A. A., Reid, I. N., Golimowski, D. A., and Ivezić, Ž.: 2010, *AJ* **139**, 2679
- Casagrande, L., Portinari, L., and Flynn, C.: 2006, *MNRAS* **373**, 13

- Cayrel, R.: 1988, in G. Cayrel de Strobel and M. Spite (eds.), *The Impact of Very High S/N Spectroscopy on Stellar Physics*, Vol. 132 of *IAU Symposium*, p. 345
- Chaplin, W. J., Kjeldsen, H., Christensen-Dalsgaard, J., Basu, S., Miglio, A., Appourchaux, T., Bedding, T. R., Elsworth, Y., García, R. A., Gilliland, R. L., Girardi, L., Houdek, G., Karoff, C., Kawaler, S. D., Metcalfe, T. S., Molenda-Żakowicz, J., Monteiro, M. J. P. F. G., Thompson, M. J., Verner, G. A., Ballot, J., Bonanno, A., Brandão, I. M., Broomhall, A.-M., Bruntt, H., Campante, T. L., Corsaro, E., Creevey, O. L., Doğan, G., Esch, L., Gai, N., Gaulme, P., Hale, S. J., Handberg, R., Hekker, S., Huber, D., Jiménez, A., Mathur, S., Mazumdar, A., Mosser, B., New, R., Pinsonneault, M. H., Pricopi, D., Quirion, P.-O., Régulo, C., Salabert, D., Serenelli, A. M., Silva Aguirre, V., Sousa, S. G., Stello, D., Stevens, I. R., Suran, M. D., Uytterhoeven, K., White, T. R., Borucki, W. J., Brown, T. M., Jenkins, J. M., Kinemuchi, K., Van Cleve, J., and Klaus, T. C.: 2011, *Science* **332**, 213
- Christensen-Dalsgaard, J., Kjeldsen, H., Brown, T. M., Gilliland, R. L., Arentoft, T., Frandsen, S., Quirion, P.-O., Borucki, W. J., Koch, D., and Jenkins, J. M.: 2010, *ApJL* **713**, L164
- Czekala, I., Andrews, S. M., Mandel, K. S., Hogg, D. W., and Green, G. M.: 2015, *ApJ* **812**, 128
- Dekker, H., D’Odorico, S., Kaufer, A., Delabre, B., and Kotzlowski, H.: 2000, in M. Iye and A. F. Moorwood (eds.), *Optical and IR Telescope Instrumentation and Detectors*, Vol. 4008 of *Proceedings of the SPIE*, pp 534–545
- Donati, J.-F.: 2003, in J. Trujillo-Bueno and J. Sanchez Almeida (eds.), *Solar Polarization*, Vol. 307 of *Astronomical Society of the Pacific Conference Series*, p. 41
- Ducati, J. R.: 2002, *VizieR Online Data Catalog* 2237
- Favata, F., Micela, G., and Sciortino, S.: 1997, *A&A* **323**, 809
- Figueira, P., Oshagh, M., Adibekyan, V. Z., and Santos, N. C.: 2014, *A&A* **572**, A51
- Frandsen, S. and Lindberg, B.: 1999, in H. Karttunen and V. Pirola (eds.), *Astrophysics with the NOT*, p. 71
- Gonzalez, G., Carlson, M. K., and Tobin, R. W.: 2010, *MNRAS* **403**, 1368
- Gonzalez, G. and Laws, C.: 2000, *AJ* **119**, 390
- Gray, D. F.: 2005, *The Observation and Analysis of Stellar Photospheres*, 3rd ed.
- Griffin, R. and Griffin, R.: 1967, *MNRAS* **137**, 253
- Grundahl, F., Fredslund Andersen, M., Christensen-Dalsgaard, J., Antoci, V., Kjeldsen, H., Handberg, R., Houdek, G., Bedding, T. R., Pallé, P. L., Jessen-Hansen, J., Silva Aguirre, V., White, T. R., Frandsen, S., Albrecht, S., Andersen, M. I., Arentoft, T., Brogaard, K., Chaplin, W. J., Harpsøe, K., Jørgensen, U. G., Karovicova, I., Karoff, C., Kjærgaard Rasmussen, P., Lund, M. N., Sloth Lundkvist, M., Skottfelt, J., Norup Sørensen, A., Tronsgaard, R., and Weiss, E.: 2017, *ApJ* **836**, 142
- Gustafsson, B., Edvardsson, B., Eriksson, K., Jørgensen, U. G., Nordlund, Å., and Plez, B.: 2008, *A&A* **486**, 951

Hartman, J. D.: 2010, *ApJL* **717**, L138

Hartman, J. D., Bakos, G. Á., Torres, G., Kovács, G., Johnson, J. A., Howard, A. W., Marcy, G. W., Latham, D. W., Bieryla, A., Buchhave, L. A., Bhatti, W., Béky, B., Csubry, Z., Penev, K., de Val-Borro, M., Noyes, R. W., Fischer, D. A., Esquerdo, G. A., Everett, M., Szklenár, T., Zhou, G., Bayliss, D., Shporer, A., Fulton, B. J., Sanchis-Ojeda, R., Falco, E., Lázár, J., Papp, I., and Sári, P.: 2014, *AJ* **147**, 128

Hellier, C., Anderson, D. R., Cameron, A. C., Delrez, L., Gillon, M., Jehin, E., Lendl, M., Maxted, P. F. L., Pepe, F., Pollacco, D., Queloz, D., Ségransan, D., Smalley, B., Smith, A. M. S., Southworth, J., Triaud, A. H. M. J., Udry, S., and West, R. G.: 2014, *MNRAS* **440**, 1982

Hinkel, N. R., Young, P. A., Pagano, M. D., Desch, S. J., Anbar, A. D., Adibekyan, V., Blanco-Cuaresma, S., Carlberg, J. K., Delgado Mena, E., Liu, F., Nordlander, T., Sousa, S. G., Korn, A., Gruyters, P., Heiter, U., Jofré, P., Santos, N. C., and Soubiran, C.: 2016, *ApJS* **226**, 4

Hinkle, K., Wallace, L., and Livingston, W.: 1995a, *Publications of the ASP* **107**, 1042

Hinkle, K. H., Wallace, L., and Livingston, W.: 1995b, in A. J. Sauval, R. Blomme, and N. Grevesse (eds.), *Laboratory and Astronomical High Resolution Spectra*, Vol. 81 of *Astronomical Society of the Pacific Conference Series*, p. 66

Huber, D., Silva Aguirre, V., Matthews, J. M., Pinsonneault, M. H., Gaidos, E., García, R. A., Hekker, S., Mathur, S., Mosser, B., Torres, G., Bastien, F. A., Basu, S., Bedding, T. R., Chaplin, W. J., Demory, B.-O., Fleming, S. W., Guo, Z., Mann, A. W., Rowe, J. F., Serenelli, A. M., Smith, M. A., and Stello, D.: 2014, *ApJS* **211**, 2

Husser, T.-O., Wende-von Berg, S., Dreizler, S., Homeier, D., Reiners, A., Barman, T., and Hauschildt, P. H.: 2013, *A&A* **553**, A6

Jofré, P., Heiter, U., Soubiran, C., Blanco-Cuaresma, S., Worley, C. C., Pancino, E., Cantat-Gaudin, T., Magrini, L., Bergemann, M., González Hernández, J. I., Hill, V., Lardo, C., de Laverny, P., Lind, K., Masseron, T., Montes, D., Mucciarelli, A., Nordlander, T., Recio Blanco, A., Sobeck, J., Sordo, R., Sousa, S. G., Tabernero, H., Vallenari, A., and Van Eck, S.: 2014, *A&A* **564**, A133

Jones, M. I., Jenkins, J. S., Rojo, P., and Melo, C. H. F.: 2011, *A&A* **536**, A71

Jones, M. I., Jenkins, J. S., Rojo, P., Olivares, F., and Melo, C. H. F.: 2015, *A&A* **580**, A14

Kaufer, A., Stahl, O., Tubbesing, S., Nørregaard, P., Avila, G., Francois, P., Pasquini, L., and Pizzella, A.: 1999, *The Messenger* **95**, 8

Kippenhahn, R. and Weigert, A.: 1994, *Stellar Structure and Evolution*, Springer-Verlag

Kjeldsen, H. and Bedding, T. R.: 1995, *A&A* **293**, 87

Kopparapu, R. K., Ramirez, R., Kasting, J. F., Eymet, V., Robinson, T. D., Mahadevan, S., Terrien, R. C., Domagal-Goldman, S., Meadows, V., and Deshpande, R.: 2013, *ApJ* **765**, 131

Kunitomo, M., Ikoma, M., Sato, B., Katsuta, Y., and Ida, S.: 2011, *ApJ* **737**, 66

- Kupka, F. G., Ryabchikova, T. A., Piskunov, N. E., Stempels, H. C., and Weiss, W. W.: 2000, *Baltic Astronomy* **9**, 590
- Kurucz, R.: 1993, *ATLAS9 Stellar Atmosphere Programs and 2 km/s grid. Kurucz CD-ROM No. 13. Cambridge, Mass.: Smithsonian Astrophysical Observatory, 1993*. 13
- Lebzelter, T., Seifahrt, A., Uttenthaler, S., Ramsay, S., Hartman, H., Nieva, M.-F., Przybilla, N., Smette, A., Wahlgren, G. M., Wolff, B., Hussain, G. A. J., Käufel, H. U., and Seemann, U.: 2012, *A&A* **539**, A109
- Lindgren, S., Heiter, U., and Seifahrt, A.: 2016, *A&A* **586**, A100
- Mayor, M., Pepe, F., Queloz, D., Bouchy, F., Rupprecht, G., Lo Curto, G., Avila, G., Benz, W., Bertaux, J.-L., Bonfils, X., Dall, T., Dekker, H., Delabre, B., Eckert, W., Fleury, M., Gilliotte, A., Gojak, D., Guzman, J. C., Kohler, D., Lizon, J.-L., Longinotti, A., Lovis, C., Megevand, D., Pasquini, L., Reyes, J., Sivan, J.-P., Sosnowska, D., Soto, R., Udry, S., van Kesteren, A., Weber, L., and Weilenmann, U.: 2003, *The Messenger* **114**, 20
- Mayor, M. and Queloz, D.: 1995, *A Jupiter-mass companion to a solar-type star*
- McWilliam, A.: 1990, *ApJS* **74**, 1075
- Mortier, A., Santos, N. C., Sousa, S., Israelian, G., Mayor, M., and Udry, S.: 2013a, *A&A* **551**, A112
- Mortier, A., Santos, N. C., Sousa, S. G., Adibekyan, V. Z., Delgado Mena, E., Tsantaki, M., Israelian, G., and Mayor, M.: 2013b, *A&A* **557**, A70
- Mortier, A., Sousa, S. G., Adibekyan, V. Z., Brandão, I. M., and Santos, N. C.: 2014, *A&A* **572**, A95
- Neuforge-Verheecke, C. and Magain, P.: 1997, *A&A* **328**, 261
- Newton, I.: 1687, *Philosophiae Naturalis Principia Mathematica. Auctore Js. Newton*
- Ngo, H., Knutson, H. A., Hinkley, S., Bryan, M., Crepp, J. R., Batygin, K., Crossfield, I., Hansen, B., Howard, A. W., Johnson, J. A., Mawet, D., Morton, T. D., Muirhead, P. S., and Wang, J.: 2016, *ApJ* **827**, 8
- Nicholls, C. P., Lebzelter, T., Smette, A., Wolff, B., Hartman, H., Käufel, H.-U., Przybilla, N., Ramsay, S., Uttenthaler, S., Wahlgren, G. M., Bagnulo, S., Hussain, G. A. J., Nieva, M.-F., Seemann, U., and Seifahrt, A.: 2017, *A&A* **598**, A79
- Niedzielski, A., Villaver, E., Nowak, G., Adamów, M., Kowalik, K., Wolszczan, A., Deka-Szymankiewicz, B., Adamczyk, M., and Maciejewski, G.: 2016, *A&A* **588**, A62
- Nowak, G., Niedzielski, A., Wolszczan, A., Adamów, M., and Maciejewski, G.: 2013, *ApJ* **770**, 53
- Önehag, A., Heiter, U., Gustafsson, B., Piskunov, N., Plez, B., and Reiners, A.: 2012, *A&A* **542**, A33
- Piskunov, N. E., Kupka, F., Ryabchikova, T. A., Weiss, W. W., and Jeffery, C. S.: 1995, *A&A Supp.* **112**, 525
- Ramírez, I., Allende Prieto, C., and Lambert, D. L.: 2013, *ApJ* **764**, 78

- Ramírez, I., Fish, J. R., Lambert, D. L., and Allende Prieto, C.: 2012, *ApJ* **756**, 46
- Ramírez, I. and Meléndez, J.: 2005, *ApJ* **626**, 465
- Santos, N. C., Adibekyan, V., Figueira, P., Andreasen, D. T., Barros, S. C. C., Delgado-Mena, E., Demangeon, O., Faria, J. P., Oshagh, M., Sousa, S. G., Viana, P. T. P., and Ferreira, A. C. S.: 2017, *ArXiv e-prints*
- Santos, N. C., Israelian, G., and Mayor, M.: 2004, *A&A* **415**, 1153
- Santos, N. C., Sousa, S. G., Mortier, A., Neves, V., Adibekyan, V., Tsantaki, M., Delgado Mena, E., Bonfils, X., Israelian, G., Mayor, M., and Udry, S.: 2013, *A&A* **556**, A150
- Sato, B., Izumiura, H., Toyota, E., Kambe, E., Ikoma, M., Omiya, M., Masuda, S., Takeda, Y., Murata, D., Itoh, Y., Ando, H., Yoshida, M., Kokubo, E., and Ida, S.: 2008, *PASJ* **60**, 539
- Sato, B., Omiya, M., Harakawa, H., Izumiura, H., Kambe, E., Takeda, Y., Yoshida, M., Itoh, Y., Ando, H., Kokubo, E., and Ida, S.: 2012, *PASJ* **64**
- Sato, B., Omiya, M., Harakawa, H., Liu, Y.-J., Izumiura, H., Kambe, E., Takeda, Y., Yoshida, M., Itoh, Y., Ando, H., Kokubo, E., and Ida, S.: 2013, *PASJ* **65**
- Smiljanic, R., Korn, A. J., Bergemann, M., Frasca, A., Magrini, L., Masseron, T., Pancino, E., Ruchti, G., San Roman, I., Sbordone, L., Sousa, S. G., Tabernero, H., Tautvaišienė, G., Valentini, M., Weber, M., Worley, C. C., Adibekyan, V. Z., Allende Prieto, C., Barisevičius, G., Biazzo, K., Blanco-Cuaresma, S., Bonifacio, P., Bragaglia, A., Caffau, E., Cantat-Gaudin, T., Chorniy, Y., de Laverny, P., Delgado-Mena, E., Donati, P., Duffau, S., Franciosini, E., Friel, E., Geisler, D., González Hernández, J. I., Gruyters, P., Guiglion, G., Hansen, C. J., Heiter, U., Hill, V., Jacobson, H. R., Jofre, P., Jönsson, H., Lanzafame, A. C., Lardo, C., Ludwig, H.-G., Maiorca, E., Mikolaitis, Š., Montes, D., Morel, T., Mucciarelli, A., Muñoz, C., Nordlander, T., Pasquini, L., Puzeras, E., Recio-Blanco, A., Ryde, N., Sacco, G., Santos, N. C., Serenelli, A. M., Sordo, R., Soubiran, C., Spina, L., Steffen, M., Vallenari, A., Van Eck, S., Villanova, S., Gilmore, G., Randich, S., Asplund, M., Binney, J., Drew, J., Feltzing, S., Ferguson, A., Jeffries, R., Micela, G., Negueruela, I., Prusti, T., Rix, H.-W., Alfaro, E., Babusiaux, C., Bensby, T., Blomme, R., Flaccomio, E., François, P., Irwin, M., Koposov, S., Walton, N., Bayo, A., Carraro, G., Costado, M. T., Damiani, F., Edvardsson, B., Hourihane, A., Jackson, R., Lewis, J., Lind, K., Marconi, G., Martayan, C., Monaco, L., Morbidelli, L., Prisinzano, L., and Zaggia, S.: 2014, *A&A* **570**, A122
- Snedden, C. A.: 1973, *Ph.D. thesis*, THE UNIVERSITY OF TEXAS AT AUSTIN.
- Soubiran, C., Le Campion, J.-F., Brouillet, N., and Chemin, L.: 2016, *A&A* **591**, A118
- Sousa, S. G., Santos, N. C., Adibekyan, V., Delgado-Mena, E., and Israelian, G.: 2015, *A&A* **577**, A67
- Sousa, S. G., Santos, N. C., Israelian, G., Mayor, M., and Monteiro, M. J. P. F. G.: 2007, *A&A* **469**, 783
- Sousa, S. G., Santos, N. C., Israelian, G., Mayor, M., and Udry, S.: 2011, *A&A* **533**, A141
- Sousa, S. G., Santos, N. C., Mayor, M., Udry, S., Casagrande, L., Israelian, G., Pepe, F., Queloz, D., and Monteiro, M. J. P. F. G.: 2008, *A&A* **487**, 373
- Takeda, Y., Sato, B., and Murata, D.: 2008, *PASJ* **60**, 781

- Torres, G., Andersen, J., and Giménez, A.: 2010, *Astronomy and Astrophysics Reviews* **18**, 67
- Torres, G., Winn, J. N., and Holman, M. J.: 2008, *ApJ* **677**, 1324
- Tsantaki, M., Andreasen, D. T., Teixeira, G. D. C., Sousa, S. G., Santos, N. C., Delgado-Mena, E., and Bruzual, G.: 2017, *MNRAS* **555**, A150
- Tsantaki, M., Sousa, S. G., Adibekyan, V. Z., Santos, N. C., Mortier, A., and Israelian, G.: 2013, *A&A* **555**, A150
- Valenti, J. A. and Piskunov, N.: 1996, *A&A Supp.* **118**, 595
- Wolszczan, A. and Frail, D. A.: 1992, *Nature* **355**, 145
- Zieliński, P., Niedzielski, A., Wolszczan, A., Adamów, M., and Nowak, G.: 2012, *A&A* **547**, A91